Detection of continuous gravitational wave signals: pattern tracking with the Hough Transform

M.Alessandra Papa*, Bernard F. Schutz*,
Sergio Frasca‡† and Pia Astone†

* *Max-Planck-Institut für Gravitationsphysik*
Albert Einstein Institut
Schlaatzweg 1, D-14473 Potsdam, Germany

‡ *Dip. di Fisica, Univ. di Roma "La Sapienza"*
P.le A. Moro 2, 00185 Roma, Italy

† *INFN Sez. di Roma I*
P.le A. Moro 2, 00185 Roma, Italy

Abstract.
Searching for patterns originating from continuous signals in time-frequency diagrams – such diagrams are produced by the very first states of a hierarchical procedure which are described in [2] – is the issue that we shall address in this presentation. We shall outline the main features of a strategy based on the use of the Hough transform by presenting the concept with an easy example and then illustrating the way we will apply it to the specific continuous gravitational wave signal search.

INTRODUCTION

The aim of the procedure we shall outline here is that of identifying candidate continuous signals in the data from a gravitational wave detector by means of a procedure acting on spectra computed on a suitable time stretch. The motivation for this incoherent analysis is that computational time constraints make it necessary to investigate alternative strategies to coherent matched filtering for all-sky all-frequencies searches [1].

The basic idea is that a low signal to noise (snr hereafter) signal will not show up as a significant peak in one of the short spectra. But still, if a signal is there, the occurence of the same peak in many spectra may acquire significance and help the detection. So, the strategy consists of two steps: the first step when one selects peaks and produces time-frequency diagrams [2], the second when one finds in these diagrams patterns which are consistent with the expected time evolution of the istantaneous frequencies of the searched signals. The latter is the issue addressed in this presentation.

PATTERN TRACKING

Fig. 1 shows a typical time frequency diagram. In it, a few signal points are hidden, but, due their "low density", it is not possibile to tell which they are by simple visual inspection. A specific pattern tracking technique must thus be implemented which is capable of operating in such low snr conditions. A promising one is based on the use of the Hough transform (HT, hereafter): "*the Hough transform is recognized as being a powerful tool in shape analysis which gives good results even in the presence of noise and occlusion*"([4]). This is a transformation from the space of the data points to the space of the parameters describing the signals one is looking for. Therefore, is relies on the a-priori knowledge of the searched shape. The Hough transform was invented by Paul V.C. Hough in the early sixties ([3]) in order to identify particle tracks in bubble chambers

CP456, *Laser Interferometer Space Antenna*
edited by William M. Folkner
 1-56396-848-7/98/$15.00

of high energy physics experiments ([5]). Since then, a great deal of work has been done on the subject – see review paper by Leavers ([4]) – with the scope of improving the performance of the Hough transform at detecting complex shapes embebbed in noise while overcoming the growing computational and storage cost that must be paid for growing number of parameters.

The basic idea of the HT is rather simple and we shall explain it by means of an easy example. Suppose one knows that in a set of *(x,y)* points, such as those shown in the left panel of fig. 1, a subset that follows a linear law (y=ax+b) is hidden and that one wants to estimate the parameters a and b. A way to do this is to set a grid on one of the parameters, say b_j, and then, for each data point (x_i, y_i), by inversion, find the corresponding a_{ij}. One can then set a grid also on the parameter a and tell how many counts fall in each pixel[1] of the resulting (a, b) plane: $x(a_i, b_j)$. The claim is that all the signal points will add up coherently in the same pixel, corresponding to the right value of the parameters, whereas noise points will be randomly scattered in the plane[2]. So, by studying the clustering properties of the maps in the space of parameters it is possibile to give an estimate of the right parameter values and of the corresponding false alarm probability. In fig.2 the panel on the right shows the map obtained by Hough transforming the data set of fig.1 for the searched linear behaviour. The maximum clustering takes place in the pixel $a = 1, b = 0$ which actually corresponds to the correct values of the parameters of the signal. The inversion does not, though, produce a uniform histogram: there will be pixels that are more likely to have higher counts than others just by chance and this appears clearly in the left plot of fig. 2 where the expected value of the count in each pixel for noise only (estimated over 50 trials) is colour coded. In order to be able to compare the outcomes in different pixels, we can "normalize" this variable to its expected value and standard deviation in order to make it indipendent of the particular pixel one is looking at and to define a measure of the contrast with respect to the expected mean. Thus we define a new variable

$$t(a_i, b_j) = \frac{x(a_i, b_j) - \mu(a_i, b_j)}{\sigma(a_i, b_j)},$$

where $\sigma(a_i, b_j)$ can be estimated from $\mu(a_i, b_j)$ by noting that $x(a_i, b_j)$ is a variable that follows a binomial distribution with probability $p \simeq \frac{\mu}{N}$, where N is the number of trials performed to estimate μ. Figure 3 shows the map for this new variable. The most significant pixel found is that corresponding to the signal, namely the $(a = 1, b = 0)$ pixel with $t = 4.59$, even though not at a very high overall significance level, which is about 30% (false alarm probability to have the value of $t = 4.59$ in any pixel of the map). Improvements can be obtained by using a finer grid on a and b. In the absence of errors in the position of the data points, in fact, using a finer grid in the parameter space enhances the significance of the clustering in the signal pixel simply because the expected noise in the pixels decreases with pixel area. The grid that was used in the example

---

1) In the language of HTs pixels are usually refered to as "accumulator cells".

2) And also signal points inverted for "wrong" values of the parameters.

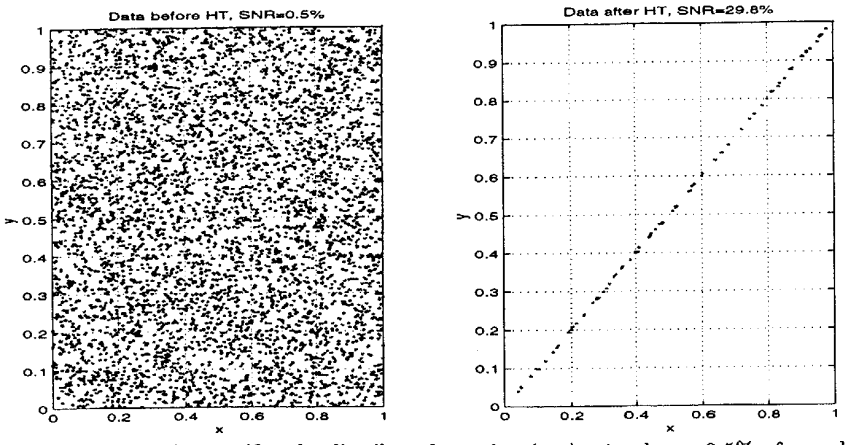

FIGURE 1. Left plot: 5000 points uniformly distributed on the *(x,y)* axis plus a 0.5% of couples that follow un unknown linear law. The density of signal points is so low that it is not possible to guess where they are by visual inspection. Right plot: the selected data after Hough filtering cointain a much higher fraction of signal, round 30%.

was just about the coarsest one could set to barely detect a signal at SNR = 0.5%. If one were actually doing an analysis, one would then isolate the candidates points contributing to the most significant pixels (in this case a threshold could be placed, say, around $t = 4$) and then repeat the HT on a finer grid around the pixel parameter values and for the selected points only. With such a hierarchy of HTs one would improve SNR and significance of a putative signal. In practice, there is a limit to how well one can perform because usually there is an uncertainty in the position of signal points so, if the grid in the parameters becomes much finer than the uncertainty induced on these by the data error, this will cause the signal in the HT plane to be smeared out in different pixels thus decreasing SNR. Understanding optimal grid setting is a crucial step in optimizing HT performance.

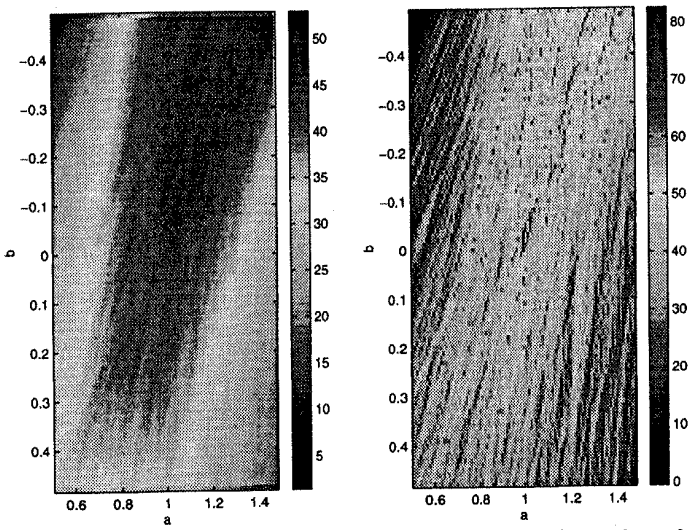

FIGURE 2. Left plot: expected Hough transform histogram for noise only (μ) in a bounded (a, b) plane. Right plot: Hough transform histogram, x, color coded in the plane of the parameters (a, b).

In the context of tracking patterns in time-frequency diagrams, the HT that must be performed is more complex than the example above: even in the simplified source case that we are studying now, the signal shape is more complicated than a linear law and the problem is not static. To start with, we have restricted our analysis to the case that the istantaneous intrinsic frequency of the source may be considered constant and that its apparent variation is due to the relative motion between the source and the detector on Earth. Under these assumptions, three parameters completely describe a signal: two celestial coordinates for the position of the source – say its right ascension α and declination δ – and its intrinsic frequency, f_0. The scheme that we are following to implement the HT is the following: set a grid of trial intrinsic frequencies and a grid on δ. For each point in the diagram – f_{ij} at time t_i and in the j-th frequency bin – the inversion yields two possibile values of α. As a matter of fact, one gets an equation in α and δ that describes a curve in the (α, δ) plane, thus what we really do, is to increment the count in the corresponding pixels. It turns out that it is most convenient to work in ecliptic coordinates and in these coordinates one finds that the curves are ellipses, (λ, β), with the center at latitude $\simeq 0$. The time t_i determines the position of the center of this ellipse and, for a given time, the "radius" depends on the distance between f_{ij} and f_0. At different times, the f_{ij}s originating from the same source will generate different circles all intersecting in a point, which identifies the position of the source. This way a map of the clustering over the whole sky is produced. Its features depend on the time scale covered by the data. For the circles to be spread with maximum uniformity, a year must be considered, but uniformity is not necessary for the analysis to work. Also note that *not* 1 year of effective observation is necessary, but only that the FFTs that we are using are spread during one year. The chance probability of the clustering count in every bin is computed as follows: the expected average value of the clustering count, μ_{ij}, for a given observation time, can easily be estimated, e.g. numerically. Then, this is used to compute the chance probability of the outcomes of the observations because the number of counts in each pixel is a random variable that follows a Poisson distribution with expected value μ_{ij}. For a year of observation, for example, μ_{ij} does not depend on the longitude of the source and we have verified that the number count follows a Poisson

distribution, at least for latitutes $|\beta| < 75°$. So it is possible to associate to each pixel its Poisson probability thus constructing such probability maps for each trial f_0. A threshold must then be set in order to select candidate sources, i.e. triplets (β, λ, f_0), that will undergo further processing.

We have implemented this HT algorithm and we are testing it on simulated spectral data (figs. 4 and 5 show the count map and the probability map for 200 spectra over 1 year). Optimal performance, as defined in [2], has not yet been reached as the implementation still needs some "fine tuning". For example, as already mentioned above, it is crucial to establish optimal gridding. In our problem this is related to the uncertainty in the definition of the frequencies f_{ij} and f_0, due to the finite resolution of the spectra. In fact, while performing the HT, we are not inverting for the actual istantaneous frequency of the signal, but for its discretized counterpart. This produces errors in the resulting position ellipse: it is as though the ellipse gained "a width" in the (λ, β) plane. Moreover, this width varies with time and position, making it difficult to set an a priori optimal grid. The HT scheme that we have outlined here seems particularly suited to take into account these effects quite naturally: for example, for every f_{ij}, a weight can be given to pixels neighbouring the ellipse according to the expected error on the position, at each time, induced by frequency discretization in the time-frequency diagrams. This should largely cure degradation of snr due to the choice of a non optimal gridding with a minor additional processing cost. Moreover, clustering properties in the sky maps seem to be little sensitive to small (of order 5 frequency frequency bins) deviations from the correct value of f_0, thus making it possible to search, at first, on a coarse grid in f_0 space and save computational time. Finally, points of ellipses of different radius could be weighted differently in order to construct more uniform count maps and make the statistical evaluation of the outcomes of the analysis more straightforward to interpret.

These are the issues that we are currently investigating in order to optimizate the HT scheme which we think is a promising approach for incoherent searches of continuous gravitational wave signals.

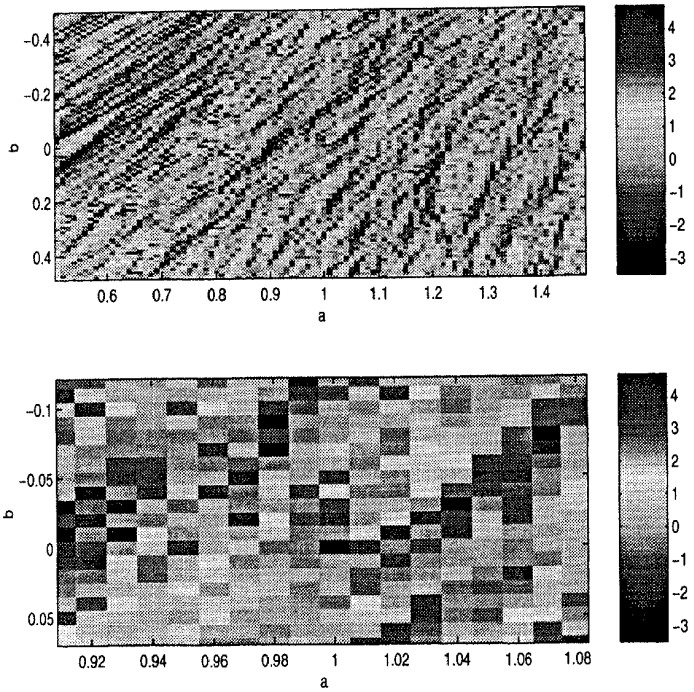

FIGURE 3. t, color coded in the plane of the parameters (a, b). The bottom figure is a zoom - near the correct values - of the map above. The most significant value for t actually occurs in the correct $a = 1, b = 0$ pixel with a value of $t = 4.59$.

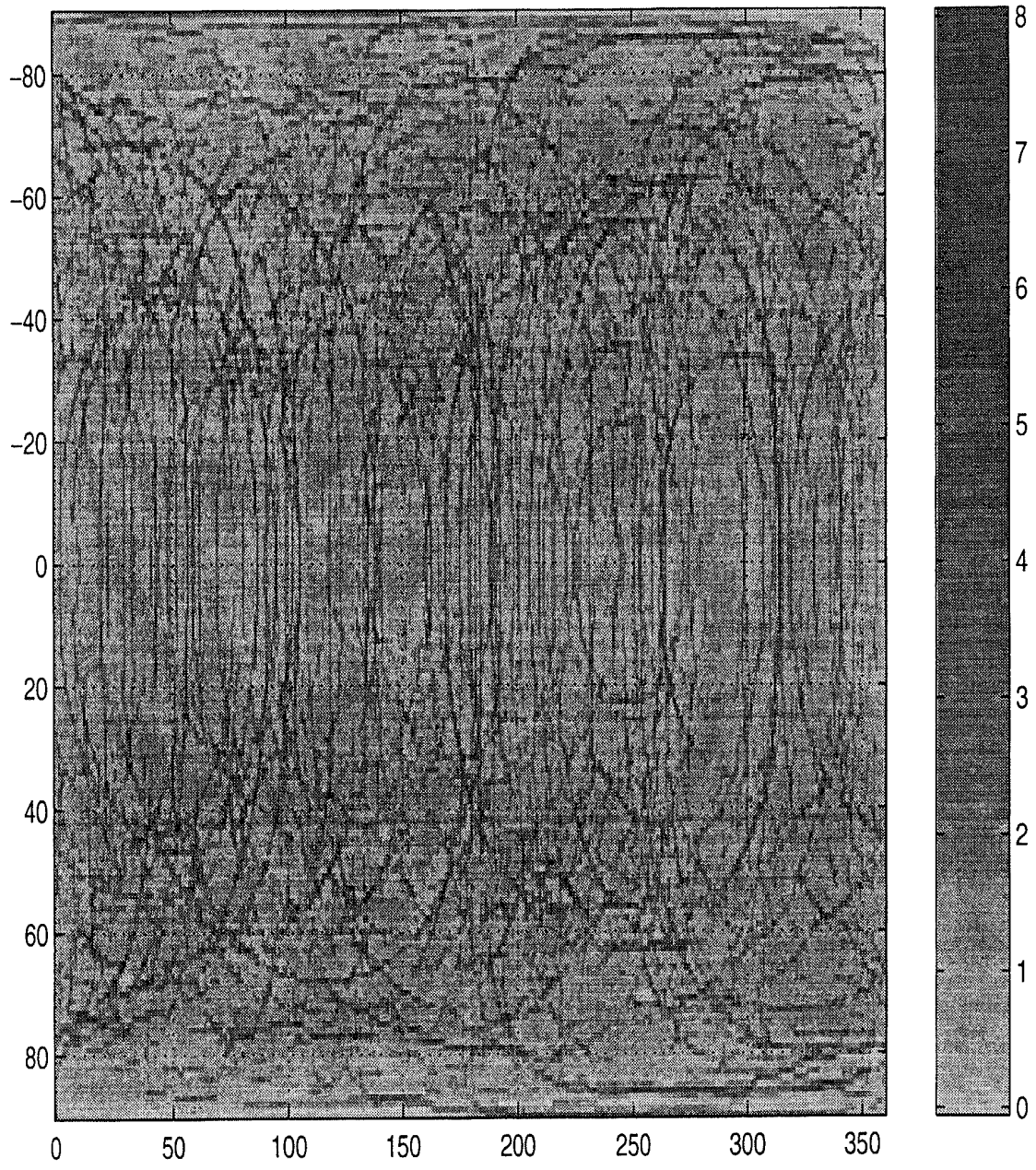

FIGURE 4. Map of the number counts for noise only for 200 spectra over one year, no signal present. The maximum clustering count is 8.

ACKNOWLEDGMENTS

We thank Prof. Lucia Zanello for having suggested to investigate the Hough transform method.

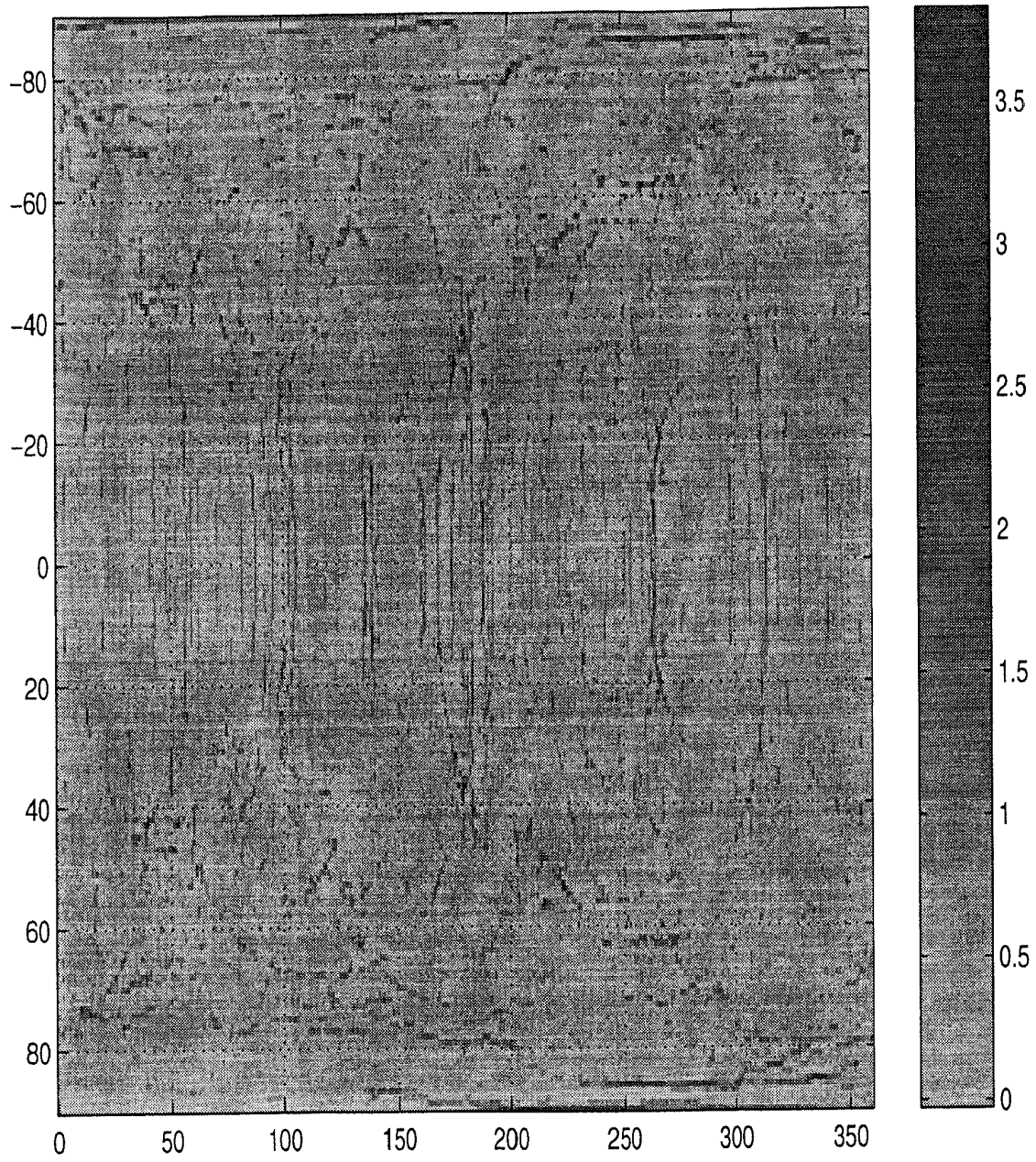

FIGURE 5. Probability map (-log10 color coded)corresponding to the clustering count map of the previous figure (no signal). The most significant value of the probability is $10^{-3.8}$ and it stands in the pixel $\lambda = 40.5, \beta = 42.5$.

REFERENCES

1. Brady P.R., Creighton T., Cutler C. and Schutz B.F "searching for periodic sources with LIGO", *Phys. Rev. D*, **57**, 4, 2101-2115, (1998).
2. Papa M.A., Astone P., Frasca S. and Schutz B.F. "Searching for continuous waves by line identification " *Gravitational Wave Data Analysis Workshop II* , Orsay, November 1997 also in *Contributions from the AEI to the GWDA2 Workshop* **AEI-057**, February 1998.

3. Hough P.V.C., "Methods and means for recognizing complex patterns", *U.S. Patent No. 3069654* , 1962.
4. Leavers, V.E., "Which Hough Transform ? ", *CVGIP: Image Understanding* **58**,2, 250-264, (1993).
5. Ermolin, Y.,and Ljuslin, C. *Nucl. Instrum. Methods Phys. Res. Sect A* **A289(3)**, 592-596 (1990).